 DOI 10.1002/mnfr.201000064 *Mol. Nutr. Food Res.* 2010, *54*, 1556–1567

RESEARCH ARTICLE

Functional and proliferative effects of repeated low-dose oral administration of furan in rat liver

Angela Mally[1], Carmen Graff[1], Olga Schmal[1], Sabrina Moro[1], Carolin Hamberger[1], Ute M. Schauer[1], Jens Brück[2], Sibel Özden[1], Max Sieber[1], Ulrich Steger[3], Dieter Schrenk[2], Gordon C. Hard[4], James Kevin Chipman[5] and Wolfgang Dekant[1]*

[1] Department of Toxicology, University of Würzburg, Germany
[2] University of Kaiserslautern, Kaiserslautern, Germany
[3] Department of Surgery, University of Würzburg, Würzburg, Germany
[4] Private Consultant, Tairua, New Zealand
[5] School of Biosciences, The University of Birmingham, Birmingham, UK

Received: February 3, 2010
Revised: March 19, 2010
Accepted: March 25, 2010

Scope: Furan, a food contaminant formed during heat processing, induces hepatocellular tumors in rodents and high incidences of cholangiocarcinomas in rats even at the lowest dose (2 mg/kg b.w.) administered. Initial estimates suggested that human intake of furan may be as high as 3.5 μg/kg b.w./day, indicating a relatively narrow margin of exposure. The aim of this study was to establish dose–response data for cytotoxicity, regenerative cell proliferation and secondary oxidative DNA damage in livers of male F344 rats treated with furan at doses $\leq$2 mg/kg b.w. for 28 days.

Methods and results: No significant signs of hepatotoxicity other than a mild, dose-dependent increase in serum cholesterol and unconjugated bile acids, and no evidence of oxidative DNA damage were seen. Histopathological alterations and proliferative changes were restricted to subcapsular areas of the left and caudate liver lobes.

Conclusion: Although statistically significant effects were only seen at the 2 mg/kg b.w. dose during the course of our study, a ~two and ~threefold increase in 5-bromo-2′-deoxyuridine labeling index was observed at 0.1 and 0.5 mg/kg b.w., respectively, suggesting that chronic exposure to doses even below 2 mg/kg b.w. may cause proliferative changes in rat liver and highlighting the need to assess furan carcinogenicity at lower doses.

Keywords:
Carcinogenicity / Cell proliferation / Furan / liver

1 Introduction

In 2004, a survey by the US Food and Drug Administration (FDA) revealed the presence of the chemical *furan* in a variety of foods that undergo heat treatment, such as coffee, canned and jarred foods including baby food, http://www.cfsan.fda.gov/~dms/furandat.html. Furan, which is widely used as an industrial chemical, is a potent hepatotoxicant and liver carcinogen in rodents. In a 2-year bioassay conducted by the National Toxicology Program (NTP), furan was reported to cause a significant increase in hepatocellular adenomas and carcinomas in male and female B6C3F1 mice and male Fischer 344 rats and high incidences of cholangiocarcinomas in rats of both sexes (Table 1) [1]. Importantly, tumor induction with high incidences was shown to occur even at the lowest doses administered (2 and 8 mg/kg b.w. in rats and mice, respectively) [1].

Correspondence: Dr. Angela Mally, Department of Toxicology, University of Würzburg Versbacher Str. 9, 97078 Würzburg, Germany
E-mail: mally@toxi.uni-wuerzburg.de
Fax: +49-931-20148865

Abbreviations: 8-oxo-dG, 8-oxo-7,8-dihydro-2′-deoxyguanosine; **BrdU,** 5-bromo-2′-deoxyuridine; **CK,** creatinine kinase; **H&E,** hematoxylin and eosin; **OPLS-DA,** orthogonal projection to latent structure-discriminant analysis; **PCA,** principle component anaylsis

*Current address: Department of Pharmaceutical Toxicology, Faculty of Pharmacy, Istanbul University, Istanbul, Turkey

Table 1. Incidence of liver tumors in the 2-year carcinogenicity study in F344 rats [1]

	Dose (mg/kg b.w.)			
	0	2	4	8
Male				
Cholangiocarcinoma	0/50	43/50	48/50	49/50
Hepatocellular adenoma and carcinoma	1/50	5/50	22/50	35/50
Female				
Cholangiocarcinoma	0/50	49/50	50/50	48/50
Hepatocellular adenoma and carcinoma	0/50	2/50	4/50	8/50

Initial exposure estimates based on the food consumption data and the occurrence of furan in various food items suggested that dietary intake levels may be as high as 3.5 μg/kg b.w./day [2], raising concern that the presence of furan in food may present a potential risk to human health. Although more recent exposure assessments in Europe and the US indicated somewhat lower furan intakes for adult consumers (EU-median: 0.78 μg/kg b.w./day, 95th percentile: 1.75 μg/kg b.w./day; US-mean: 0.26 μg/kg b.w./day, 90th percentile: 0.61 μg/kg b.w./day) and infants (EU-simulated high exposure for 6–9 month-old infants: 1.14–1.34 μg/kg b.w./day; US-mean: 0.41 μg/kg b.w./day, 90th percentile: 0.99 μg/kg b.w./day), the presently available data on furan levels in food are still limited (*e.g.* lack of data on furan content in home-cooked food) and may thus not present a suitable indicator of actual furan intake *via* food. However, it appears that there may be a relatively narrow margin (1000–2000) between the estimated human exposure and doses, which causes high incidences of liver tumors in rodents by unknown mechanisms.

Hepatotoxic effects of furan are thought to be mediated by bioactivation. Furan is oxidized by cytochromes P450 (presumably *via* formation of an epoxide intermediate) to yield a chemically reactive α,β-unsaturated dialdehyde, *cis*-2-butene-1,4-dial, which has been suggested to act as the key metabolite responsible for furan toxicity and carcinogenicity [3, 4]. *In vitro* studies demonstrate that *cis*-2-butene-1,4-dial covalently modifies nucleosides [5, 6] and amino acid residues [7], suggesting that both genotoxicity (*via* formation of DNA adducts) and chronic cytotoxicity mediated through binding of *cis*-2-butene-1,4-dial to critical target proteins may play a role in the mechanism of tumor formation by furan. However, standard *in vitro* genotoxicity tests have generated inconsistent results [1, 4, 8, 9], and while induction of micronuclei was recently reported in cytokinesis-blocked splenocytes of mice treated with furan [10], the important question of whether or not furan forms DNA adducts *in vivo* has not been fully resolved [2].

Irrespective of its genotoxic potential, however, work by Wilson *et al.* [11] has provided evidence to suggest that increased cell proliferation secondary to furan-induced hepatocyte necrosis is a key event in the carcinogenic response to furan. Administration of furan to male and female F344 rats at the highest bioassay dose of 8 mg/kg b.w. for 1, 3 and 6 wk resulted in a significant increase in hepatocyte labeling index at all time points examined. Proliferative changes were accompanied by subcapsular focal areas of inflammation and small foci of necrosis/inflammation within the hepatic parenchyma [11]. The link between sustained cytotoxicity, compensatory proliferation and furan-induced tumor formation was further supported by a recent study in female mice [12]. In addition, previous work demonstrating a marked increase in 8-oxo-7,8-dihydro-2′-deoxyguanosine (8-oxo-dG) at sites associated with furan-induced hepatocyte necrosis [13] indicates that secondary oxidative DNA damage resulting from cytotoxicity and chronic inflammation – coupled with enhanced cell turnover – may contribute to furan carcinogenicity. When the dose level is sufficient to cause both centrilobular and periportal necrosis, this can lead to irrecoverable metaplasia and cholangiofibrosis which continues to expand, even after cessation of furan treatment, and is accompanied by a persistent chronic inflammatory infiltrate [14].

While these studies have considerably improved our understanding of early events associated with furan tumorigenicity, it needs to be emphasized that – with the exception of a study in female mice – relatively high doses of furan associated with significant hepatotoxicity (8 mg/kg b.w. and above) were applied. Considering the presence of high incidences of liver tumors in rats at the lowest dose tested (2 mg/kg b.w.), and the apparent narrow margin of exposure, there is a strong need to establish dose–response data at relatively low dose levels as a basis for risk assessment of human furan exposures *via* the food. The objective of this study was to assess furan hepatotoxicity, associated oxidative DNA damage and proliferative changes after repeated oral administration of furan at a known carcinogenic dose and doses closer to human exposure.

2 Materials and methods

2.1 Chemicals

Furan (Cas-No. 110-00-9) (≥99% puritiy) was obtained from Aldrich (Taufkirchen, Germany, Product number 185922). Corn oil (C8267) and 5-bromo-2′-deoxyuridine (BrdU) were purchased from Sigma, (Taufkirchen, Germany). Cholic acid

(CA), ursodeoxycholic acid (UDCA), lithocholic acid (LCA) and sodium taurocholate hydrate (TCA) were obtained from Fluka (Taufkirchen, Germany). Hyodeoxycholic acid (HDCA), chenodeoxycholic acid (CDCA), deoxycholic acid (DCA), sodium taurohyodeoxycholate hydrate (THDCA), sodium taurochenodeoxycholate (TCDCA), sodium taurodeoxycholate (TDCA), sodium taurolithocholate (TLCA), sodium glycocholate (GCA), sodium glycochenodeoxycholate (GCDCA) and sodium glycodeoxycholate (GDCA) were obtained from Sigma. Sodium tauroursodeoxycholate (TUDCA), sodium glycoursodeoxycholate (GUDCA) and sodium glycolithocholate (GLCA) were obtained from Calbiochem (Germany). The tetradeuterated internal standard, 2,2,4,4-d_4-cholic acid was obtained from Isotec (*via* Sigma-Aldrich, Taufkirchen, Germany), HPLC grade methanol and ACN were from Sigma-Aldrich Fluka. Purified water for LC-MS/MS was purchased from Roth (Karlsruhe, Germany). Unless otherwise indicated, all other chemicals were from Sigma-Aldrich Fluka, Merck (Darmstadt, Germany) or Roth.

2.2 Animals

All animal experiments were performed according to national animal welfare regulations after authorization by the local authorities (Regierung von Unterfranken). Male F344/N rats (6–7 wk old) were purchased from Harlan-Winkelmann, Borchen, Germany. Animals were housed into groups of five (respectively three for the satellite group) in Macrolon cages with wire mesh tops and standard softwood bedding and allowed free access to pelleted standard rat maintenance diet (SSNIFF, Soest, Germany) and tap water. Room temperature was maintained at $22 \pm 2^{\circ}C$ with a relative humidity of $55 \pm 10\%$ and a day/night cycle of 12 h. Food and water consumption were recorded twice weekly. All animals were observed twice daily for clinical signs of toxicity, and body weight measurements were conducted twice *per* week. Rats were allowed to acclimatize for 7 days prior to the furan treatment. Due to the high volatility of furan, dosing solutions were prepared daily immediately prior to administration as previously described [1, 12]. For the main study, rats ($n = 5$ *per* dose and time point) were administered furan dissolved in corn oil (4 mL/kg b.w.) at doses of 0, 0.1, 0.5 and 2 mg/kg b.w. by gavage for 28 days (9 am, 5 days *per* week), with an interim sacrifice after 5 days of treatment. An off-dose recovery group (0 and 2 mg/kg b.w. dose groups only) was kept for additional 2 wk (recovery period) after the end of the 4-wk treatment period. For urine collection, animals were transferred into metabolic cages 24 h prior to necropsy. Animals were fasted for 24 h, but allowed free access to drinking water. An aliquot of urine was immediately used for clinical chemistry analyses. The remaining urine was aliquoted and stored at $-20^{\circ}C$ until further analysis. Animals were killed by CO_2 asphyxiation, and blood was collected by cardiac puncture into heparinized tubes for clinical chemistry and bile acid analyses. Blood samples were centrifuged and plasma was stored at $-20^{\circ}C$. Livers were removed, weighed, and separated into the liver lobes. Aliquots of each liver lobe were fixed in 10% neutral buffered formalin for histopathological evaluation. The remaining parts were aliquoted, flash frozen in liquid nitrogen, and stored at $-80^{\circ}C$.

For cell proliferation studies, satellite groups ($n = 3$ *per* dose and time point) were treated as described above. Five days prior to sacrifice, osmotic minipumps (ALZET, 2ML1, flow rate 9.8 µL/h; Charles River Laboratories, Sulzfeld, Germany) containing 2 mL of a sterile solution of BrdU (15 mg/mL in PBS, pH 7.4) were subcutaneously implanted into the dorsal thoracic region under Ketamine (90 mg/kg b.w., i.p.)/Xylazine (10 mg/kg b.w. i.p.) anaesthesia to allow incorporation of BrdU into newly synthesized DNA. The animals were housed separately after the insertion of the pumps. At sacrifice, aliquots from the left, median, and caudate lobe were fixed in formalin and subsequently embedded in paraffin. Sections were cut at 4 µm and processed for BrdU and apoptosis labeling, as well as for routine hematoxylin & eosin (H&E) staining.

2.3 Urine analysis and clinical chemistry

Routine clinical chemistry analyses in plasma were carried out at the Laboratory for Clinical Chemistry, University of Würzburg on a Vitros 700XR (Ortho-Clinical Diagnostics, Neckargemünd) using the standard protocols for the determination of these parameters according to the manufacturer's instructions.

2.4 Cell proliferation

Cell proliferation in livers was assessed using the BrdU technique. BrdU-positive cells in liver were visualized on formalin-fixed paraffin-embedded sections by using the BrdU *in situ* detection kit (BD Biosciences, Heidelberg, Germany) according to the manufacturer's instructions. Slides were blind coded and cell proliferation was determined by light microscopic counts of hepatocytes, which acquired brown nuclear staining *per* total number of hepatocytes. Initially, 18 fields on each liver section were used to determine the hepatocellular BrdU labeling index throughout the liver parenchyma. On each section, a minimum of 1500 cells were counted at $400 \times$ magnification. Quantification of BrdU labeling in 24 randomly selected subcapsular regions was performed using an ocular grid overlying sections viewed at $400 \times$ magnification to delineate areas covering a defined distance from the surface into the hepatic parenchyma (~eight rows of hepatocytes). On each section, ~1500 cells were counted.

2.5 Apoptosis

The TUNEL assay was performed on 5-µm paraffin sections to label fragmented DNA in apoptotic cells using the

FragEL™ DNA Fragmentation Detection Kit (Oncogene) according to the manufacturer's instructions. Labeled cells were counted as described for cell proliferation above.

2.6 Determination of 8-oxo-7,8-dihydro-2′-deoxyguanosine by LC-MS/MS

8-Oxo-dG was determined as previously described in detail [15, 16]. Briefly, DNA was isolated from frozen liver tissue (left lobe) by the Nucleobond® method (Macherey-Nagel, Dueren, Germany) according to the manufacturer's instructions with minor modifications (modified elution buffer: 1.5 M NaCl, 0.05 M Tris, 15% ethanol, pH 7.0), hydrolyzed by nuclease P1 and alkaline phosphatase and analyzed on an Agilent 1100 series LC coupled to a triple stage quadrupole mass spectrometer (API 3000, Applied Biosystems, Darmstadt, Germany) equipped with a TurboIon® Spray source. As 2′-deoxyguanosine can be oxidized to 8-oxo-dG during ESI resulting in overestimation of 8-oxo-dG concentrations in biological samples containing excess 2′-deoxyguanosine, mass transitions for 2′-deoxyguanosine (*m/z* 268–152) were monitored during the sample analysis to confirm chromatographic separation of 8-oxo-dG and 2′-deoxyguanosine.

2.7 Metabonomics

Detailed descriptions of ^{1}H-NMR and MS-based metabonomics approaches including statistical analyses applied in our laboratory have recently been published [17]. For GC-MS analysis, proteins were precipitated from 50 μL urine by the addition of 100 μL ice-cold methanol. After centrifugation (14 000 rpm, 10 min), 50 μL of the supernatant was transferred into a GC vial and evaporated to dryness, derivatized with 50-μL methoxyamine hydrochloride in pyridine (20 mg/mL) at 40°C for 90 min, silylated at 40°C for 1 h with 100 μL *N*-methyl-*N*-(trimethylsilyl)-trifluoracetamide, and analyzed on a HP6980 gas chromatograph with split/splitless inlet (split ratio 20:1) equipped with a J&W Scientific DB5-MS column (dimensions: 30 m × 0.25 mm × 0.1 μm film) coupled to a HP5973 mass selective detector. Data recording and machine control were performed by HP Chemstation version D.02.00. Samples were introduced by a CombiPal autosampler. Inlet temperature and transfer line temperatures were set to 280°C. The oven temperature increased from 60 to 250°C at a rate of 30°C/min and held at 250°C for 5 min. Helium carrier gas flow was kept constant at 0.8 mL/min. The detector was switched off during the elution of the urea signal from 11.50 to 16.00 min. The detector operated in the scan mode from 60 to 650 *m/z* with a sampling rate of 1 leading to 8.69 scans/s and a threshold of 50 counts. Source temperature and quadrupole temperatures were kept at 230 and 150°C, respectively. Chromatograms were exported in the platform-independent netCDF (*.cdf) format with the ChemStation export function for further analysis. Automatic peak detection and peak alignment were performed by the freely available software XCMS version 1.6.1. The results table containing mass spectral features as mass/retention time pairs in a tab-separated text file (*.txt) was imported into Excel work sheets. Normalization to TIC and further data handling steps such as sorting the data according to retention time was carried out in Excel prior to multivariate data analysis with SIMCA-P version 11.5 (Umetrics, Umeå, Sweden).

For LC-MS analysis, urine samples were thawed, centrifuged at 14 000 × *g* and 4°C for 10 min and diluted to an equal osmolality of 154 mosmol/kg (final volume 150 μL). An LC-MS analysis was run on an UPLC system coupled to a Micromass LCT Premier (ESI-TOF) controlled by MassLynx software version 4.1. The analytical column was an ACQUITY BEH C18 (2.1 × 100 mm, 1.7 μm) and kept at 40°C (Waters GmbH, Eschborn, Germany). An injection volume of 10 μL was used with a flow rate of 0.500 mL/min. Solvents were water with 0.1% formic acid (solvent A) and ACN with 0.1% formic acid (solvent B) with the following gradient: 0 min 100% A, 4.00 min 80% A, 9.00 min 5% A, 12.00 min 100% A. The following MS parameters were used: negative ionization mode; survey scan mass range 50–1000 Da; nebulization gas 700 L/h at 450°C; cone gas 15–20 L/h; source temperature 120°C; capillary voltage 60 V; LCT-W optics mode with 12 000 resolution using dynamic range extension; data acquisition rate 0.1 s with a 0.01 s interscan delay; lock spray 2000 counts; lock spray method: leucine/enkephalin 50 fmol/μL, lock mass: *m/z* 556.2771, flow rate: 30 μL/min, frequency: 5 s; data collection was performed in centroid mode averaged over ten scans. Raw data files were exported in the platform-independent netCDF (*.cdf) format with the MassLynx export function for further analysis. Automatic peak detection and peak alignment were performed using XCMS version 1.11.20, and results table containing mass spectral features as mass/retention time pairs in a tab-seperated text file (*.txt) was exported to SIMCA P+version 11.5 for multivariate data analysis.

For ^{1}H-NMR metabonomics, solids were removed by centrifugation (14 000 rpm, 10 min) and 630 μL of urine were buffered with 70 μL of a 1 M phosphate buffer in D_2O containing 10 mM d_4-trimethylsilylpropionic acid sodium salt as shift lock reagent. ^{1}H-NMR spectra were recorded on a Bruker DMX 600 spectrometer equipped with a 5-mm DCH cryoprobe using pulsed magnetic field gradients (both by Bruker Biospin GmbH, Rheinstetten, Germany). Water suppression was achieved with the noesygppr1d pulse sequence from the Bruker library. For each spectrum, 32 scans were recorded. Each spectrum was manually baseline-corrected and referenced to d_4-trimethylsilylpropionic acid sodium salt ($\delta = 0.00$ ppm). The spectra were then imported into the Chenomx NMR Suite 4.6 (Chenomx, Edmonton, Canada) and binned into 0.04-ppm wide bins. After removal of bins associated with water resonance from

4.40 to 6.20 ppm, binned NMR data were normalized to total integral and imported into SIMCA-P version 11.5. for a multivariate data analysis.

For the multivariate data analysis, variables were mean-centered and pareto-scaled for principle component anaylsis (PCA) and orthogonal projection to latent structure-discriminant analysis (OPLS-DA). The significance of the components was determined by leave-one-out cross validation, the default validation tool in SIMCA P+11.5. Only significant components were used for the analysis.

2.8 Bile acid analysis

Following SPE of bile acids from rat plasma, bile acid analysis was performed according to a previously published LC-MS/MS method, which allows simultaneous determination of a range of individual bile acids and their respective glycine and taurine conjugates [18]. Proteins were precipitated from 100-μL plasma samples by addition of 100 μL ice-cold ethanol containing 2.4 μM 2,2,4,4-d_4-cholic acid as an internal standard and centrifugation for 30 min at 14 000 rpm and 4°C. The supernatant was removed and diluted with 800-μL 0.1 M sodium phosphate buffer (pH 7.0). The mixture was passed through a Chromabond C_{18} SPE cartridge (3 mL, 200 mg; Macharey-Nagel, Düren, Germany), preconditioned with 3 mL methanol and 3 mL water. After adsorption of the sample, the cartridge was washed with 3 mL water and dried under vacuum. Bile acids were eluted with 2 × 3 mL methanol. The eluate was evaporated to dryness under a gentle stream of nitrogen at 40°C and redissolved in 200 μL of mobile phase. Aliquots (10 μL) of each sample were injected into the LC-MS/MS system for analysis. LC-MS/MS analysis was performed on an Agilent 1100 series LC coupled to an API 3000 triple quadrupole mass spectrometer (Applied Biosystems). Samples were injected into the LC-MS/MS system through an Agilent 1100 series autosampler. Separations were carried out on a Synergi 4 μ Fusion-RP 80, (2.0 mm × 150 mm; 4 μ, 100 A; column fitted with a security guard column system (Phenomenex, Aschaffenburg, Germany). The samples were separated by gradient elution with 20 mM ammonium acetate buffer (pH 8.0) (solvent A) and ACN:methanol (3:1, v/v) (solvent B) using the following conditions: 75% A, linear gradient to 60% A in 30 min, followed by a second linear gradient to 30% A in 15 min, then linear increase to 75% A in 5 min and isocratic at 75% for 10 min at a flow-rate of 0.2 mL/min. The API 3000 mass spectrometer was operated with a Turbo Ion Spray source in the negative ion mode with a voltage of −4000 V. Spectral data were recorded with N_2 as the heater gas at 400°C and as the collision gas (CAD = 4) in the multiple reaction-monitoring mode (MRM) with a dwell time of 50 ms for each mass transition. The following mass transitions were used as quantifier and qualifiers, respectively. CA (*m/z* 407→343; 407→407; 407→289); UDCA (*m/z* 391→391; 391→373); HDCA (*m/z* 391→391; 391→373); CDCA (*m/z* 391→391; 391→373); DCA (*m/z* 391→391; 391→345; 391→/373); LCA (*m/z* 375→375); TCA (*m/z* 514→80; 514→124); TUDCA (*m/z* 498→80; 498→124); THDCA (*m/z* 498→80; 498→124); TCDCA (*m/z* 498→80; 498→124); TDCA (*m/z* 498→80; 498→124); TLCA (*m/z* 482→80; 482→124); GCA (*m/z* 464→74; 464→402); GUDCA (*m/z* 448→74; 448→386); GCDCA (*m/z* 448→74; 448→386); GDCA (*m/z* 448→74; 448→386; 448→402); GLCA (*m/z* 432→74; 432→388); CA-d_4 (*m/z* 411→347).

Calibration curves were linear in the range of 0.01–2 μM for UDCA, HDCA, DCA, TCA, THDCA, TCDCA, TDCA and GCA, 0.01–1 μM for CDCA, 0.001–0.2 μM for TUDCA, TLCA, GUDCA, GCDCA, GDCA and GLCA, 0.02–2 μM for CA and LCA. Detection limits for individual bile acid ranged from 0.2 to 10 nM. CA, UDCA, CDCA, GUDCA and GLCA were below the limit of detections in all samples. Recoveries from spiked samples (0.02 and 0.2 μM for each bile acid; $n = 4$) were >85%.

2.9 Statistical analyses

Unless otherwise indicated, data are expressed as mean ± SD. Statistical analyses were performed using one-way ANOVA followed by Dunnett's *post-hoc* test. A *p*-value < 0.05 was considered statistically significant.

3 Results

3.1 Body and organ weight

Treatment with furan at doses of 0, 0.1, 0.5 and 2 mg/kg b.w. for 4 wk had no effect on food and drinking water consumption (data not shown), and no clinical signs of toxicity were observed. No treatment-related changes in body and relative liver weights were evident throughout the study (Table 2).

3.2 Clinical chemistry and bile acid analysis

Oral administration of furan had no significant effects on clinical chemistry parameters in plasma or urine except for a slight decrease in glucose and alkaline phosphatase activity in high-dose animals after 4-wk treatment, which were not considered to be of toxicological relevance, and a small, but dose-dependent increase in cholesterol following 4-wk treatment with furan (Table 2). This effect returned to control levels after the 2-wk recovery period. No increase in liver enzymes indicative of hepatic injury was observed throughout the study (Table 2). To obtain further information on potential hepatobiliary effects of furan, a highly sensitive LC/MS-MS method was used for the analysis of six individual bile acids and their respective glycine and taurine conjugates following SPE of bile acids from rat plasma. A slight but statistically significant increase in the concentrations of the unconjugated bile acids DCA and HDCA was observed in plasma of rats treated with furan at 2 mg/kg b.w. for 4 wk as compared to

Table 2. Clinical chemistry, body and relative organ weight after repeated administration of 0, 0.1, 0.5 and 2 mg/kg b.w. furan for 28 days

	Dose (mg/kg b.w.)			
	0	0.1	0.5	2
Body and organ weight				
Body weight initial (g)	125.2±6.3	124.8±4.4	126.6±9.8	136.9±5.6
Body weight final (g)	208.5±8.7	207.5±9.7	199.4±13.7	212.6±14.3
Relative liver weight (%)	3.4±0.1	3.2±0.1	3.1±0.04**	3.3±0.1
Clinical chemistry				
Glucose (mg/dL)	164±12	153±6	150±12	138±20*
Creatinine (mg/dL)	0.3±0.1	0.2±0.1	0.3±0.1	0.3±0.1
Urea (mg/dL)	30.9±3.0	29.4±1.7	30.3±1.6	34.2±2.4
Total bilirubin (mg/dL)	0.0±0.0	0.02±0.05	0.02±0.05	0.02±0.05
Aspartate aminotransferas (U/L)	134±19	132±36	142±56	168±105
Alanine aminotransferase (U/L)	53.5±5.2	58.8±10.0	67.0±29.2	81.1±57.9
Glutamate dehydrogenase 9U/L)	6.4±0.7	7.4±2.0	8±3.2	11.2±7.2
γ-Glutamyl transferase (U/L)	1.6±0.7	2.2±1.6	1.6±0.9	1.9±1.0
Alkaline phosphatase (U/L)	320±35	278±20*	259±6**	264±7.8**
Lactate dehydrogenase (U/L)	303±78	255±155	330±216	457±521
Creatinine kinase total (U/L)]	1177±300	982±760	1004±580	1344±1350
Cholesterol (mg/dL)	48.6±3.8	49.4±3.2	53.6±2.7	56.0±3.5**
Triglycerides (mg/dL)	39.4±9.3	59.6±9.6*	53.6±10.6	49.6±7.6
Total protein (g/dL)	6.9±0.2	6.62±0.22	6.7±0.26	6.9±0.2
Bile acids				
Unconjugated				
HDCA (μM)	0.83±0.21	0.73±0.04	1.09±0.26	1.95±0.95**
DCA (μM)	0.13±0.03	0.13±0.05	0.23±0.08	0.48±0.21**
Total (μM)	0.96±0.24	0.86±0.05	1.31±0.31	2.43±1.12**
Taurine conjugates				
TCA (μM)	0.77±0.42	0.40±0.18	0.68±0.22	0.98±0.31
THDCA (μM)	1.99±0.33	1.09±0.26	1.52±0.57	2.45±1.11
TDCA (μM)	0.40±0.19	0.31±0.09	0.44±0.20	0.59±0.14
TLCA (μM)	0.01±0.00	0.01±0.00	0.01±0.00	0.01±0.00
TCDCA (μM)	0.24±0.07	0.15±0.04	0.21±0.07	0.21±0.04
TUDCA (μM)	0.01±0.00	0.01±0.00	0.01±0.01	0.02±0.01
Total (μM)	3.42±0.95	1.97±0.49	2.87±0.98	4.25±1.44
Glycine conjugates				
GCA (μM)	0.60±0.33	0.26±0.12	0.29±0.20	0.31±0.29
GCDCA (μM)	0.02±0.01	0.01±0.01	0.01±0.01	0.01±0.01
GDCA (μM)	0.06±0.01	0.04±0.01	0.04±0.03	0.05±0.03
Total (μM)	0.68±0.33	0.31±0.13	0.34±0.23	0.37±0.33
Ratio unconjugated/conjugated	0.24±0.06	0.39±0.09	0.44±0.15	0.54±0.24*

Data are presented as mean±SD of five individual animals *per* dose group. Statistical analysis was performed by ANOVA and Dunnett's *post-hoc* test. Statistically significant changes are indicated by $^{*}p<0.05$ and $^{**}p<0.01$.

controls (Table 2), which returned to control levels after 2-wk recovery (data not shown).

3.3 Metabonomic analyses

Metabonomics, *i.e.* the multicomponent analysis of the biochemical composition of body fluids combined with statistical models, has been recognized as a powerful and sensitive tool to detect toxicity [19]. In this study, we applied a combination of ^{1}H-NMR, GC-MS and LC-MS techniques to identify metabolic perturbations in rats exposed to furan. However, oral administration of furan did not induce changes in the biochemical composition of urine, as determined by a lack of separation of control from treated animals by unsupervized PCA of GC-MS data (Fig. 1A). Analysis of urine samples by LC-MS in both negative and positive ionization modes also did not reveal metabolic changes in response to furan treatment using unsupervized PCA with both unit variance and pareto (par) scaling (Figs. 1B, D). Consistent with the MS-based

metabonomics approaches, no significant changes in urine ^{1}H-NMR spectra were evident following treatment of rats with furan at doses of 0, 0.1, 0.5 and 2 mg/kg b.w. for up to 4 wk (Fig. 1C). Similar to PCA, supervized OPLS-DA did not give rise to models with significant components (Supporting Information Figs. 1 and 2).

3.4 Histopathology, apoptosis and cell proliferation

Light microscopic evaluation of H&E-stained liver sections of caudate and left liver lobes, which had previously been shown to be most susceptible to furan toxicity in rats [11], did not reveal marked histopathological changes in response to furan treatment. Few apoptotic cells were seen in the various exposed livers, but at similar frequency as in the control livers. These observations were supported by quantitative analysis based on the TUNEL assay. Consistent with previous reports, the apoptotic index, expressed as the percentage of TUNEL-positive hepatocytes throughout the liver parenchyma, was below $<0.1\%$ in all dose groups, and no treatment-related changes were evident (data not shown).

Time- and dose-related effects of furan on cell proliferation were assessed following 5-day administration of BrdU *via* osmotic minipumps. No effects on the biliary epithelium were apparent, and initial counting of BrdU-labeled hepatocytes throughout the liver parenchyma did not reveal statistically significant changes in cell proliferation in furan treated animals as compared to controls (Fig. 2 and Figs. 3A, B). However, increased BrdU labeling was observed in subcapsular areas of the left and caudate lobes of rats exposed to furan (Fig. 2). Determination of the BrdU labeling index specifically within these areas revealed a dose-dependent increase in the number of proliferating hepatocytes (Figs. 3C, D), which was evident in the more susceptible caudate lobe even within 5 days of furan treatment. Although statistically significant

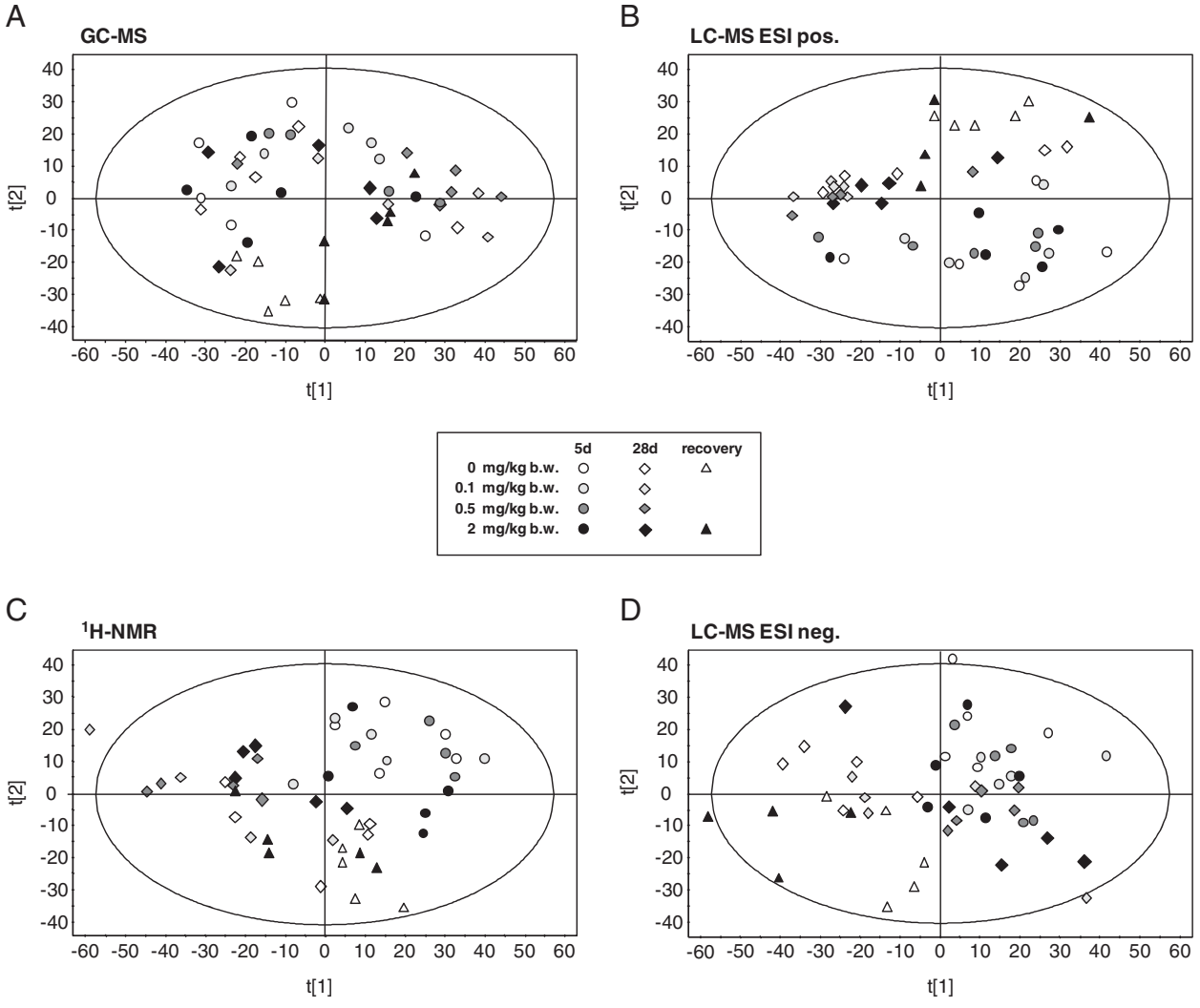

Figure 1. Principal component analysis (unit variance-scaled) of GC-MS (A) and LC-MS data in both the positive (B) and negative (D) ionization mode, and ^{1}H-NMR data (C).

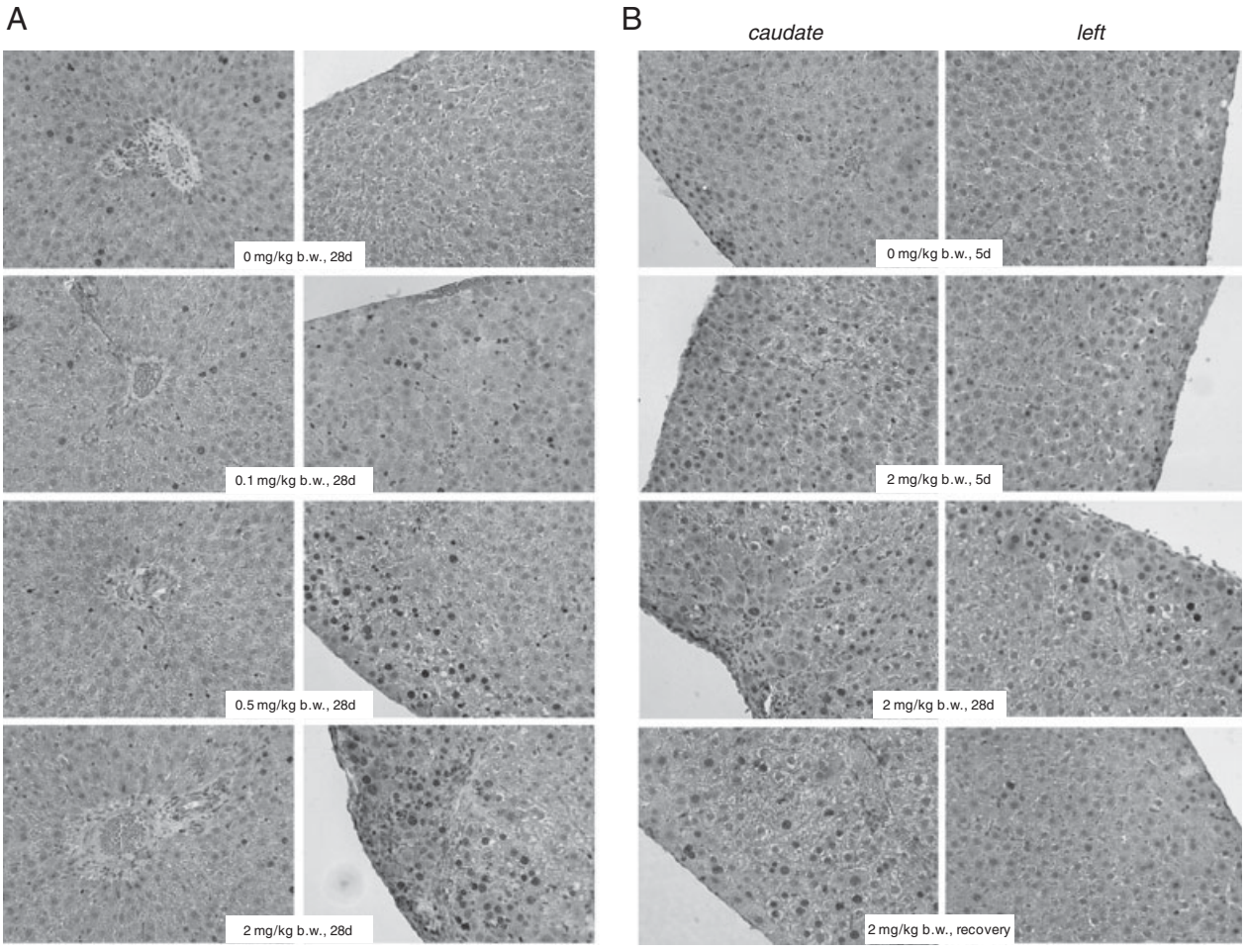

Figure 2. (A) Representative images of periportal (left panel) and subcapsular (right panel) regions showing dose-dependent proliferative changes restricted to subcapsular focal areas in the caudate liver lobe of furan treated rats. (B) Time-dependent changes in hepatocyte cell proliferation in subcapsular surface lesions in the caudate and left liver lobe in response to furan at 2 mg/kg b.w., showing reduced BrdU labeling after the 2-wk recovery period as compared with earlier time points. BrdU-positive cells were visualized on formalin-fixed paraffin-embedded sections using an anti-BrdU antibody.A colour version of this figure is available as supplemental online information.

changes were restricted to rats treated with furan at 2 mg/kg b.w., a ~two-fold and ~three-fold increase in BrdU index above background was observed in the low- (0.1 mg/kg b.w.) and mid- (0.5 mg/kg b.w.) dose group, respectively. Increased mitotic activity in these locations was accompanied by an occasional apoptotic cell and very thin foci of nonspecific inflammation, evidenced by a slight accumulation of mononuclear cells. After the 14-day recovery period, BrdU labeling indices in both left and caudate liver lobes of rats dosed with furan regressed as compared with the 28-day time point, reaching control levels in the left liver lobes.

3.5 Oxidative DNA damage

As furan has previously been shown to induce oxidative DNA lesions at high doses (30 mg/kg b.w.) as evidenced by increased levels of 8-oxo-dG [13], formation of 8-oxo-dG in rat liver in response to furan was assessed by LC-MS/MS. In contrast to high-dose treatment, determination of 8-oxo-dG in this study revealed no significant changes in 8-oxo-dG between controls and furan-exposed rats (Table 3).

4 Discussion

For many carcinogens operating primarily by a nongenotoxic mode of action, a close correlation between sustained cell proliferation – either compensatory to cell toxicity or involving loss of growth regulation – and tumorigenicity has been established [20, 21]. In contrast to genotoxic carcinogens, for which no tolerable exposure levels can be defined, it is assumed that certain nongenotoxic carcinogens at doses below the threshold for cytotoxicity do not pose a cancer risk [22]. Although the potential role of furan genotoxicity *in vivo* has not been satisfactorily addressed to date [2], this and

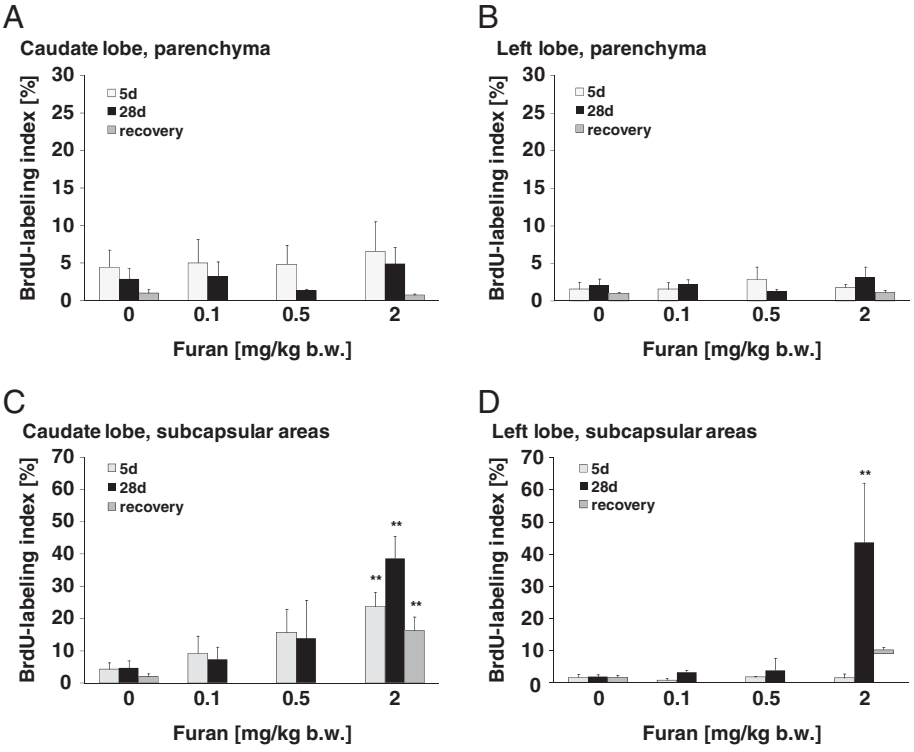

Figure 3. BrdU labeling index in the caudate (A, C) and left (B, D) liver lobe following repeated administration of furan. (A, B) parenchyma, (C, D) subcapsular areas. Data are presented as mean ± SD ($n = 3$ animals/group). Statistical analysis was performed by ANOVA followed by Dunnett's *post-hoc* test. Statistically significant changes compared with controls are indicated as $^{*}p < 0.05$, $^{**}p < 0.01$.

previous studies demonstrate that hepatocellular proliferation is an early response to furan at doses which cause liver tumors in rodents.

In our study, which was designed to establish dose–response data for cytotoxicity, regenerative cell proliferation and secondary oxidative DNA damage in rat liver at a known carcinogenic dose and doses closer to estimated human exposure to furan *via* food, histopathology and routine clinical chemistry provided little evidence for hepatotoxicity following treatment of male F344 rats with furan at 0, 0.1, 0.5 and 2 mg/kg b.w. for up to 28 days. Similarly, PCA and OPLS-DA models constructed with GC-MS, LC-MS and NMR metabonomics data could not separate treated from control animals, indicating that 28-day treatment with furan did not induce significant metabolic changes in urine which may reflect liver toxicity. However, analysis of individual bile acids in serum, which has been shown to be a sensitive indicator of hepatic injury [23], revealed a significant increase in unconjugated bile acids as opposed to taurine and glycine conjugates at 2 mg/kg b.w.. These changes were consistent with the small increase in cholesterol after 4-wk treatment and suggest that furan may alter hepatobiliary function. Although we cannot conclude at present whether these effects are due to impaired hepatobiliary transport, interference with bile acid biosynthesis or depletion of free amino acids due to reaction with *cis*-2-butene-1,4-dial, it is interesting to note that teucrin A, a hepatotoxic furan-containing diterpenoid found in the herb germander, was recently shown to form covalent protein adducts with bile acid CoA:amino acid *N*-acyltransferase [24], an enzyme

Table 3. 8-Oxo-dG/10^6 dG levels in liver DNA following treatment with furan, indicating that furan did not induce oxidative DNA damage under the conditions of this study. Data are presented as mean ± SD of five individual animals *per* dose group

Treatment time	8-Oxo-dG/10^6 dG			
Dose	0 mg/kg b.w.	0.1 mg/kg b.w.	0.5 mg/kg b.w.	2.0 mg/kg b.w.
5 days	5.8 ± 1.2	4.9 ± 0.7	4.9 ± 1.4	4.4 ± 1.3
28 days	5.0 ± 1.0	5.5 ± 1.7	6.2 ± 1.8	5.2 ± 1.4
Recovery	4.9 ± 0.2	–	–	4.9 ± 0.4

Statistical analysis was performed by ANOVA and Dunnett's *post-hoc* test. Statistically significant changes are indicated by $^{*}p < 0.05$ and $^{**}p < 0.01$.

responsible for catalyzing the conjugation of bile acids with both glycine and taurine. Considering that biotransformation of teucrin A gives rise to an 1,4-enedial derivative structurally similar to *cis*-1,4-butene-dial, it is tempting to speculate that bile acid CoA:amino acid *N*-acyltransferase may also be a target protein of furan reactive metabolites, leading to reduced ability of furan treated rat liver to conjugate and hence excrete bile acids. Unconjugated bile acids are surface-active substances which may induce necrosis *via* damage to biological membranes, but are also known to cause mitochondrial dysfunction and apoptosis [25]. Thus, hepatic accumulation of unconjugated bile acids may contribute to furan mediated hepatocellular injury.

In addition to these functional alterations, BrdU labeling revealed foci of increased hepatocyte proliferation along the edge of the left and caudate liver lobes, indicating that short-term furan administration may induce focal proliferative changes in rat liver in the absence of significant hepatotoxicity. This is in line with a report by Wilson *et al.* [11] in which furan administered to male F344 rats at the highest bioassay dose of 8 mg/kg b.w. for up to 6 wk was found to induce substantial cell proliferation (18- to 51-fold increase over combined controls) without changes in liver associated plasma enzymes, suggesting that BrdU labeling may be a more sensitive indicator of response. Importantly, however, we found evidence for subcapsular hepatocyte proliferation and associated changes in the expression of cell–cycle-related genes [26] even in the low-dose range for which no tumor data are yet available. Considering the close link between cell proliferation and tumorigenesis, these findings suggest that chronic administration of furan at doses as low as 0.1 mg/kg b.w. may enhance tumor formation in rat liver and highlight the need to assess furan carcinogenicity in rats at doses well below 2 mg/kg b.w.. This appears to be particularly important as a recent study in female B6C3F1 mice has shown a significant increase in tumor incidence at a lower dose (4 mg/kg b.w.) than previously examined (8 and 15 mg/kg b.w.) in mice [12].

In contrast to studies in rats, however, low levels of hepatotoxicity induced by furan in mice were not associated with increased tumor incidence. While significant hepatic cytotoxicity was evident at doses of 1 and 2 mg/kg b.w., compensatory cell proliferation, preneoplastic and neoplastic lesions were only increased at doses $\geq$4 mg/kg b.w., but not at 1 and 2 mg/kg b.w. [12]. Thus, it appears that in mice a certain degree of tissue damage must be exceeded in order for tumor formation to occur. It is important to point out that significant species differences also exist with respect to the tumor type induced by furan, with hepatocellular adenomas and carcinomas occuring in mice and cholangiocarcinoma as the predominant tumor type in rats. A mechanistic basis for these species differences has not been established, and short-term studies in rats and mice demonstrate that the initial damage caused by furan appears to be identical in both species, with necrosis, inflammatory cell infiltration, proliferation and fibrotic changes developing from the subcapsular visceral surface and extending into the parenchyma. However, with continuing exposure the response to these lesions and thus the final outcome seems to vary between species, as bile duct proliferation, which is thought to play a critical role in the development of the cholangiocarcinomas, was subsequently observed in rats, but not in mice [11].

In rats administered relatively high doses of furan, it was recently shown that bile duct proliferation occurs in severely affected areas within the parenchyma, but not in regions where proliferation of surviving hepatocytes was apparently sufficient to replace necrotic cells [14]. Proliferating biliary ducts extended from the portal tracts into the injured parenchyma, where they started to differentiate into hepatocytes. These observations suggest that proliferation of biliary cells in rats occurs secondary to hepatocyte damage as part of a repair process to compensate for the cell loss. In most severely injured areas, however, expanding ductal cells acquired an intestinal rather than hepatocellular phenotype prior to the appearance of intestinal metaplasia [14], suggesting that the normal repair process was perturbed.

Based on these findings, one might hypothesize that the threshold for hepatocyte proliferation may not be the same as that for carcinogenicity, with tumors developing only when the capacity for adaptive repair is overwhelmed by high doses or sustained exposure to furan [27] or following irretrievable hepatocyte loss associated with proliferative metaplasia and cholangiofibrosis [14]. Thus, we cannot predict whether the proliferative changes seen in rats at low doses and in the absence of measurable DNA oxidation within 28 days will ultimately develop into tumors following chronic exposure. However, it is also important to point out that the question whether or not furan binds to DNA *in vivo* is yet to be resolved and that longer exposure periods may lead to oxidative damage *via* inflammation. It is well established that a sustained increase in cell proliferation may serve to convert DNA damage into permanent mutations; thus DNA damage and proliferation in the subcapsular regions may combine to cause neoplasia.

A mechanistic understanding of the pathogenesis of subcapsular surface lesions of specific lobes remains to be established. Based on the finding that affected areas are in close proximity to the nonglandular stomach, it has been speculated that diffusion of furan across the stomach wall may play a role [11, 27]. Alternatively, inter- and intra-lobular differences in liver perfusion or vascular lesions limiting blood supply may contribute to the regional effects, although it is unlikely that furan is exclusively delivered to these specific areas *via* the circulatory system.

In summary, our results demonstrate that short-term treatment with furan at a known carcinogenic dose and doses closer to estimated human exposure results in increased cell proliferation, specifically in subcapsular regions of target liver lobes. These findings are consistent with preliminary results from a recent 90-day toxicity study on furan using a similar dose range [28] and underscore the need to assess furan carcinogenicity in rats at lower doses than previously examined and to better understand the mechanism of action and the basis for the different tumor types that present between rats and mice. Thus, key issues which remain to be addressed include DNA adduct formation and mutagenesis *in vivo*, nongenotoxic events at longer exposures than in the present study and extending to doses to which humans are exposed, and the relationships between dose–response curves for these endpoints to better understand the contribution of genotoxic and nongenotoxic mechanisms in furan-induced tumor formation. Such information will aid risk assessment for humans.

Acknowledging the uncertainties in dose response modeling from the presently available tumor data, Carthew *et al.*

recently applied the MoE approach based on an estimated $BMDL_{10}$ of 1.28 mg/kg b.w./day for hepatocellular adenoma and carcinoma in male rats, resulting in MoEs of 750 to 4300 for exposures of infants and adults and thus well below the MoE of 10 000 considered to indicate a low priority for risk management actions [29]. Importantly, modeling of the rat cholangiocarcinoma data, the most sensitive endpoint for furan carcinogenicity, resulted in a $BMDL_{10}$ of 0.0012 mg/kg b.w./day [29] and thus an even lower MoE, further highlighting the importance of understanding the molecular events involved in the pathogenesis of this particular tumor type and its relevance to humans.

This work was supported by FP6 of the European Union (SSPE-CT-2006-44393) and DFG (MA 3323/3-1). The authors would also like to thank Caroline Kröcher, Elisabeth Rüb-Spiegel, Heike Keim-Heusler, Ursula Tatsch and Michaela Bekteshi for excellent animal care and technical assistance.

The authors have declared no conflict of interest.

5 References

[1] NTP, toxicology and carcinogenesis studies of furan (CAS No. 110-00-9) in F344 rats and B6C3F1 mice (gavage studies). *Natl. Toxicol. Program Tech. Rep. Ser.* 1993, *402*, 1–286.

[2] EFSA, Report of the Scientific Panel on Contaminants in the Food Chain on provisional findings on furan in food. *The EFSA Journal* 2004, *137*, 1–20.

[3] Chen, L. J., Hecht, S. S., Peterson, L. A., Identification of *cis*-2-butene-1,4-dial as a microsomal metabolite of furan. *Chem. Res. Toxicol.* 1995, *8*, 903–906.

[4] Peterson, L. A., Naruko, K. C., Predecki, D. P., A reactive metabolite of furan, *cis*-2-butene-1,4-dial, is mutagenic in the Ames assay. *Chem. Res. Toxicol.* 2000, *13*, 531–534.

[5] Byrns, M. C., Predecki, D. P., Peterson, L. A., Characterization of nucleoside adducts of *cis*-2-butene-1,4-dial, a reactive metabolite of furan. *Chem. Res. Toxicol.* 2002, *15*, 373–379.

[6] Byrns, M. C., Vu, C. C., Peterson, L. A., The formation of substituted 1,N6-etheno-2′-deoxyadenosine and 1,N2-etheno-2′-deoxyguanosine adducts by *cis*-2-butene-1,4-dial, a reactive metabolite of furan. *Chem. Res. Toxicol.* 2004, *17*, 1607–1613.

[7] Chen, L. J., Hecht, S. S., Peterson, L. A., Characterization of amino acid and glutathione adducts of *cis*-2-butene-1,4-dial, a reactive metabolite of furan. *Chem. Res. Toxicol.* 1997, *10*, 866–874.

[8] Kellert, M., Brink, A., Richter, I., Schlatter, J., Lutz, W. K., Tests for genotoxicity and mutagenicity of furan and its metabolite *cis*-2-butene-1,4-dial in L5178Y tk+/− mouse lymphoma cells. *Mutat. Res.* 2008, *657*, 127–132.

[9] Durling, L. J., Svensson, K., Abramsson-Zetterberg, L., Furan is not genotoxic in the micronucleus assay *in vivo* or *in vitro*. *Toxicol. Lett.* 2007, *169*, 43–50.

[10] Leopardi, P., Cordelli, E., Villani, P., Cremona, T. P. *et al.*, Assessment of *in vivo* genotoxicity of the rodent carcinogen furan: evaluation of DNA damage and induction of micronuclei in mouse splenocytes. *Mutagenesis* 2010, *25*, 57–62.

[11] Wilson, D. M., Goldsworthy, T. L., Popp, J. A., Butterworth, B. E., Evaluation of genotoxicity, pathological lesions, and cell proliferation in livers of rats and mice treated with furan. *Environ. Mol. Mutagen* 1992, *19*, 209–222.

[12] Moser, G. J., Foley, J., Burnett, M., Goldsworthy, T. L., Maronpot, R., Furan-induced dose-response relationships for liver cytotoxicity, cell proliferation, and tumorigenicity (furan-induced liver tumorigenicity). *Exp. Toxicol. Pathol.* 2009, *61*, 101–111.

[13] Hickling, K. C., Hitchcock, J. M., Oreffo, V., Mally, A. *et al.*, Evidence of oxidative stress and associated DNA damage, increased proliferative drive and altered gene expression in rat liver produced by the cholangiocarcinogenic agent furan. *Toxicol. Pathol.* 2010, *38*, 230–243.

[14] Hickling, K., Hitchcock, J. M., Chipman, J. K., Hammond, T. G., Evans, J. G., Induction and progression of cholangiofibrosis in rat liver injured by oral administration of furan. *Toxicol. Pathol.*2010, *38*, 213–229.

[15] Mally, A., Volkel, W., Amberg, A., Kurz, M. *et al.*, Functional, biochemical, and pathological effects of repeated oral administration of ochratoxin A to rats. *Chem. Res. Toxicol.* 2005, *18*, 1242–1252.

[16] Mally, A., Amberg, A., Hard, G. C., Dekant, W., Are 4-hydroxy-2(E)-nonenal derived mercapturic acids and (1)H NMR metabonomics potential biomarkers of chemically induced oxidative stress in the kidney? *Toxicology* 2007, *230*, 244–255.

[17] Sieber, M., Wagner, S., Rached, E., Amberg, A. *et al.*, Metabonomic study of ochratoxin A toxicity after repeated administration: Phenotypic anchoring enhances ability for biomarker discovery. *Chem. Res. Toxicol.* 2009, *22* 1221–1231.

[18] Ando, M., Kaneko, T., Watanabe, R., Kikuchi, S. *et al.*, High sensitive analysis of rat serum bile acids by liquid chromatography/electrospray ionization tandem mass spectrometry. *J. Pharm. Biomed. Anal.* 2006, *40*, 1179–1186.

[19] Lindon, J. C., Holmes, E., Nicholson, J. K., Metabonomics in pharmaceutical R&D. *FEBS J.* 2007, *274*, 1140–1151.

[20] Alden, C. L., Safety assessment for non-genotoxic rodent carcinogens: curves, low-dose extrapolations, and mechanisms in carcinogenesis. *Hum. Exp. Toxicol.* 2000, *19*, 557–560; discussion 571–552.

[21] Klaunig, J. E., Kamendulis, L. M., Xu, Y., Epigenetic mechanisms of chemical carcinogenesis. *Hum. Exp. Toxicol.* 2000, *19*, 543–555.

[22] Williams, G. M., Application of mode-of-action considerations in human cancer risk assessment. *Toxicol. Lett.* 2008, *180*, 75–80.

[23] Bai, C., Canfield, P. J., Stacey, N. H., Individual serum bile acids as early indicators of carbon tetrachloride- and chloroform-induced liver injury. *Toxicology* 1992, *75*, 221–234.

[24] Druckova, A., Mernaugh, R. L., Ham, A. J., Marnett, L. J., Identification of the protein targets of the reactive metabolite of teucrin A *in vivo* in the rat. *Chem. Res. Toxicol.* 2007, *20*, 1393–1408.

[25] Palmeira, C. M., Rolo, A. P., Mitochondrially-mediated toxicity of bile acids. *Toxicology* 2004, *203*, 1–15.

[26] Chen, T., Mally, A., Ozden, S., Dekant, W., Chipman, J. K., Modulation of hepatic gene expression independent of DNA methylation in furan treated F344/N Rats. *Society of Toxicology 48th Annual Meeting, Baltimore, 2009. The Toxicologist, Supplement to Toxicological Sciences* 2009.

[27] Maronpot, R. R., Giles, H. D., Dykes, D. J., Irwin, R. D., Furan-induced hepatic cholangiocarcinomas in Fischer 344 rats. *Toxicol. Pathol.* 1991, *19*, 561–570.

[28] Gill, S., Kavanagh, M., Bondy, G., Lefebvre, D. E. *et al.*, Clinical and histopathologic effects of oral furan exposure in Fischer-344 rats. *Toxicologist – J. Soc. Toxicol.* 2008, *102*.

[29] Carthew, P., DiNovi, M., Setzer, R. W., Application of the margin of exposure (MoE) approach to substances in food that are genotoxic and carcinogenic: example: furan (CAS No. 110-00-9). *Food Chem. Toxicol.* 2010, *48*, S69–S74.

